International Journal of Engineering

Journal Homepage: www.ije.ir

Numerical Studies on Performance of Helical Pile-supported Embankments Over Soft Clay

M. A. Mashayekhi, M. Khanmohammadi*

Department of Civil Engineering, Isfahan University of Technology, Isfahan, Iran

PAPER INFO

Paper history:
Received 18 September 2023
Received in revised from 16 November 2023
Accepted 26 Novermber 2023

Keywords:
Embankments
Helical Pile
Load Transfer Mechanism
Bearing Capacity
Finite Element

ABSTRACT

The need for practical and economical solutions to increase the stability of embankments and reduce their settlement is a significant issues in geotechnical engineering. An effective approach to improve the overall performance of embankment systems is using structural elements such as piles. In recent years the use of helical piles has gained consideration due to their proper performance under compressive and tensile loads, quick and easy installation, and elimination of concreting problems. This study investigates the performance of embankments supported by helical piles through a 3D numerical study using the Abaqus software. The validation was performed according to the experimental and field data provided by other researchers. Then, 3D numerical models were developed to investigate the effects of pile caps, the ratio of helix diameter to shaft diameter, the number of helices, and the optimum spacing of helices. The finite element modeling results indicated that increasing the number of helices and changing their spacing had no significant impact on controlling the settlement. It was also found that the load transfer mechanism parameters had a direct relationship with the helix dimensions and shaft diameter. Adding helices to piles increased their bearing capacity, improving parameters of the load transfer mechanism, such that the arching in a pile with three helices decreased by 40% compared to the one with one helix. The results also revealed that on average, 80% of the load imposed on a pile was sustained by the shaft, and helices had a smaller effect on the settlement of pile-supported embankments.

***doi**: 10.5829/ije.2024.37.04a.03*

Graphical Abstract

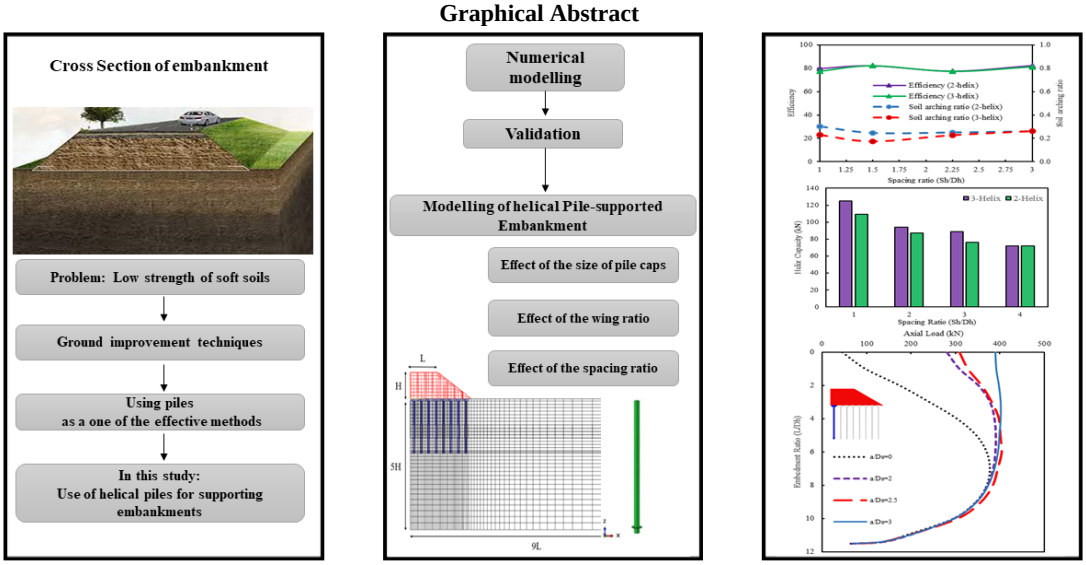

*Corresponding Author Email *mkhanmohammadi@iut.ac.ir* (M. Khanmohammadi)

Please cite this article as: Mashayekhi MA, Khanmohammadi M. Numerical Studies on Performance of Helical Pile-supported Embankments Over Soft Clay. International Journal of Engineering, Transactions A: Basics. 2024;37(04):596-607.

1. INTRODUCTION

The design and construction of road or railway embankments are not possible on problematic soils, such as soft soils, due to excessive total and differential settlements, low bearing capacity, high lateral displacement, and slope instability (1). As a rapid and economical solution, pile-supported embankments have been employed instead of traditional improvement methods of soft soils over recent years (2, 3). Studies have investigated different types of piles to be used in pile-supported embankments. Cast-in-place concrete piles (4, 5), precast concrete piles (6-8), prestressed concrete piles (9), steel piles (10, 11), deep mixed columns (12-14), stone columns (15, 16), sand-ash-gravel mixed columns (4, 17), and high-strength piles (18, 19) are some examples. Ahmed et al. (20)conducted a parametric study to simulate pile foundation and investigate its performance in soft clay. It was found that the performance of piled raft foundations on soft soils is significantly affected by the piles' spacing. When the ratio S/D exceeds 10, piles have little or no effect on the ultimate bearing capacity.

Liu et al. (21) conducted a study on different types of piles (rigid, rigid-flexible, flexible) in a pile embankment system. The results showed that the model test with rigid piles had the least settlement, while the model test with flexible piles experienced the largest settlement. However, it was found that using pile effectively reduced embankment settlement.

All types of conventional piles have specific issues such as construction problems, damaging the environment, and incurring large costs that make them deficient in some civil engineering projects.

A helical pile is a deep steel foundation system, consisting of one or more helices connected to a central shaft. The easy and rapid installation, recyclability and reusability, elimination of concreting issues, and low noises during installation are some merits of these piles, resulting in the widespread use of large-scale helical piles in industrial and building projects (22). The use of helical piles in pile-supported embankments is an alternative, whose performance evaluation requires further studies. The shaft diameter of a large-scale helical pile varies between 73 mm and 965 mm, and the diameter of the helices connected to it ranges from 152 to 1219 mm. Some references consider the ratio of helix diameter to shaft diameter between 2 and 3 (23-25). Most of the previous researches on helical piles have focused on the situation in which the piles are under direct loading, and by examining their geometric parameters, settlement performance and axial force distribution in the pile depth have been investigated and the results indicate that for cohesive soils, increasing the number of helices with the optimal distance of 1.5 times the diameter of the helix, by creating cylindrical shear, enhances pile's performance (26-28). The research on the behavior of helical piles in pile-supported embankments is limited, and further studies are required.

Based on an analysis of the technical literature, embankments are now being constructed using improvement techniques for unsuitable soils. Among these techniques, the use of piles has proven to be more effective than the others. Numerous numerical, experimental, and field investigations have been conducted using various types of piles. Therefore, the objective of this research is to investigate the performance of helical piles in pile-supprted embankment systems. In the present study, at first, a 3D finite element model of embankments supported by helical piles was verified using experimental and field data. Then, a parametric numerical study was performed to investigate the pile geometry including shaft diameter, number of helices, and width of pile cap.

1. 2. Load Transfer Mechanism The main factor governing the load transfer mechanism in pile-supported embankments is the difference between the stiffness of soil and piles and the mobilized shear strength of soil. As a result, the stress caused by the weight of embankment layers is transferred from the soft soil to the piles. Terzaghi (29) named this load transfer mechanism, the "arching effect". The arching mechanism is evaluated using the definitions of "arching ratio" and "efficiency". The arching ratio is defined as follows (30).

$$SAR = \frac{\sigma_s}{(\gamma H + q)} \quad (1)$$

In which σ_s is the stress imposed on the soil around the pile, γ is the embankment unit weight, H is the embankment height, and q is the uniform surcharge imposed on the embankment crest. The SAR ranges between zero and one. SAR = 0 indicates that the whole load caused by the embankment weight is transferred to the piles, and the arching has occurred thoroughly. On the other hand, SAR = 1 shows that no load has been transferred to piles. The efficiency parameter indicates the ratio of the load carried by piles to the load caused by the embankment weight and surcharge (31).

$$E = \frac{Q}{s^2(\gamma H + q)} \quad (2)$$

where Q equals the total forces imposed on a single pile and s is the spacing of piles. E = 0 indicates that no arching has happened, while E = 100% shows the occurrence of full arching.

Many parametric studies have been conducted on the load transfer mechanism in pile-supported embankments. Through field study and numerical studies, Hello and Villard (32) showed that increasing the pile cap width improved the efficiency of piles and reduced their

settlement. Investigating the impact of the length of floating piles on the degree of arching, Bhasi and Rajagopal (33) stated that the pile length can influence the degree of arching. Through 2D and 3D modeling of a pile-supported embankment, Ariyarathne and Liyanapathirana (34) studied the positive effect of increasing pile diameter and decreasing pile spacing on the increase in efficiency and reduction in the arching ratio. Conducting a parametric study, Meena et al. (35) showed that the elastic modulus of pile and embankment and the internal friction angle of embankment material play a vital role in the arching mechanism. Pham and Dias (36) present an extensive parametric study using three-dimensional numerical calculations for pile-supported embankments. The results indicated that the pile embankment system shows a good performance in reducing the embankment settlement. The results also suggested that the soil cohesion strengthens the arching effect, and increases the loading efficiency.

2. NUMERICAL MODELING

Figure 1 depicts a helical pile-supported embankment considered for the numerical modeling. The embankment with a height of 6 m, a crest length of 7.5m, and a lateral slope of 1:1.5 was modeled on a uniform clay layer with a depth of 30m. The steel helical piles were assumed with cylindrical sections, and the load-bearing helices were modeled as ideal disks. The effect of pile installation in the soil was ignored. In all models, the length of piles is 12m and helix diameter is fixed to 1m. In the parametric study, variables such as the dimensions of the cap width, shaft diameter, and the number of helices were considered in the modeling. During each modeling case, only one parameter was changed at a time, while keeping the other parameters at the baseline case values. The parameters and their values used in this study are summarized in Table 1. The baseline model values are presented in bold numbers. The mesh type and geometry for all the models were kept identical to eliminate the meshing size effects on the results. The meshing size was chosen to be adequately fine immediately near the piles, as well as in the contact surface between the embankment and the soft soil, and started to grow gradually with the distance from the edge of the embankment. Figure 1 depicts a sample meshing for the developed numerical model. Figure 2 demonstrates the geometry of the modeled helical pile, in which D_h and D_s denote the helix diameter and pile shaft diameter, respectively.

Regarding the boundary conditions, the displacements in the bottom boundary of the model were considered zero in three directions ($U_x = U_y = U_z = 0$). Moreover, the displacements of the model were considered zero on two sides of the model along the x-axis and on two sides of the model on the y-axis ($Ux = U_y = 0$). To model the soil and pile, 25800 eight-node elements with reduced integration (C3D8R) were used.

The embankment material was considered to be coarse-grained, and the foundation soil layer was assumed to consist of uniform soft clay with weak geotechnical properties. Moreover, since the soft clay was considered to be fully drained, the drained parameters were used. Table 2 lists the properties of the materials used in the numerical modeling. The helical pile and the pile cap were modeled in the linear elastic mode using steel and concrete materials, respectively. To model the behavior of granular embankment and soft clay medium, the Mohr-Coulomb constitutive model has been used, which gives a precise prediction of the soil behavior (37). The soil-pile behavior at their interface was defined using the friction model of Coulomb and type Penalty, in which the relative displacement equals zero until the shear stress reaches a critical value. Sliding occurs when the shear stress exceeds the shear strength. The coefficient of friction was assumed to be equal to 0.7 (38, 39).

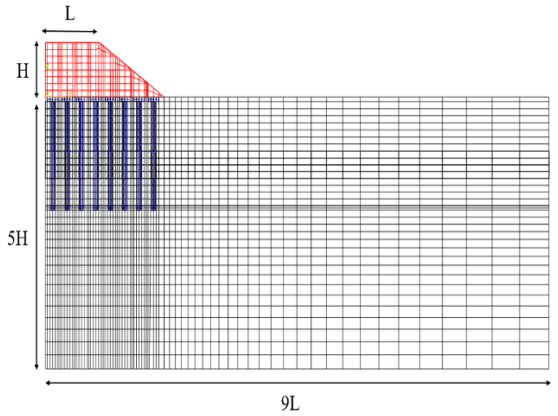

Figure 1. Schematics of the 3D model meshing

TABLE 1. Parameters values used for the parametric study

Description	Parameter	Values
Helical pile	Shaft diameter (mm)	250- **500**-667
	Depth of pile (m)	**12**
	Helix diameter (mm)	**1000**
	Number of helices	**1**-2-3
	Thickness of the shaft (mm)	**10**
	Thickness of the helix (mm)	**25**
	Vertical distance between helices (m)	1-1.5-2.25-3
	Pile spacing (m)	**2**
	Width of cap (m)	0-1-1.25-**1.5**

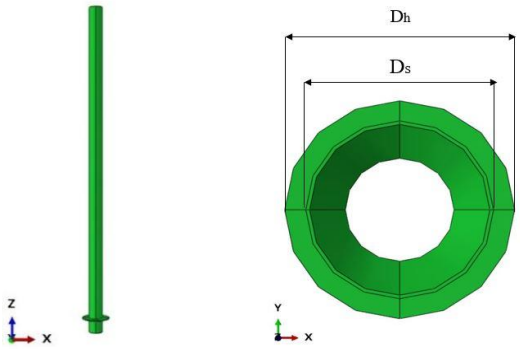

(a) (b)

Figure 2. a) Geometry of the single-helix pile, b) Cross section of the helical pile

TABLE 2. Summary of the material properties used in the finite element modeling

Material	γ (kN/m³)	E (MPa)	ν	C′ (kPa)	ϕ' (degree)	ψ (degree)
Embakment	20	60	0.3	5	30	0
Soft clay	18.4	10	0.3	8	22	0
Pile	78.5	210000	0.2	-	-	-
Cap	24	35000	0.15	-	-	-

γ = Unit weight, E = Young's modules, ν = Poisson's ratio, C = Effective cohesion, ϕ' = Effective friction angle, ψ = Dilation angle

3. VALIDATION

To validate the modeling, two studies were chosen. As the first case, the field study of TJ pile-supported embankment in China by Chen et al. (40) gives a precise description of the construction site, instrumentation, and embankment construction procedure. The cross-section of the instrumented embankment and soil profile is shown in Figure 3. The soil profile consists of a clayey soil of approximately 3m thickness underlain by a soft silty clay with a thickness of about 17m, with high water content, low permeability, and low shear strength, overlying the third layer, which is pebble. The groundwater level is at a depth of 0.5m. Figure 4 (a, b) shows a comparison between the settlement values measured in the field and the results of the numerical modeling at the soil surface and the pile cap. Comparisons of the stress at the soil surface and the pile cap are shown in Figure 5 (a, b), respectively.

The second study is based on the laboratory data in actual dimensions, related to the loading of a helical pile for the validation of numerical modeling. The helical pile modeling was validated using the data reported by Elsherbiny and El nagger (28) under compressive loading. Pile PA-1 tested in soft soil (located in northern Alberta, Canada) was chosen for the validation. The helical pile at test site A had a cylindrical shaft with one helix affixed to it. Figure 6 shows the load-displacement curves of the helical pile for both FE modeling and field test data. The comparison of the results of full-scale compressive loading at site A with the numerical results in Figure 6 indicates that validation was accurately modeled because the load-displacement response of the numerical model is in good agreement with that of the full–scale test.

Table 3 provides the chosen parameters of the piled embankment and the helical pile validation and Table 4 summarizes the piles properties.

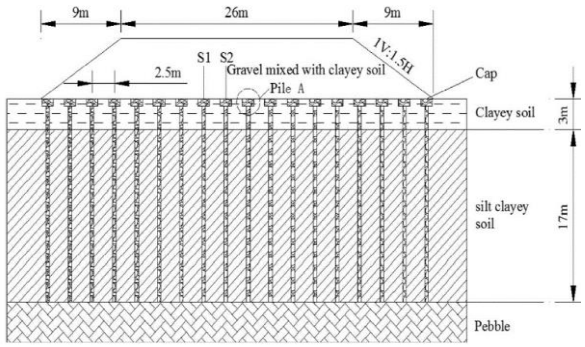

Figure 3. Cross-section of the test embankment of TJ Highway (Section G1)

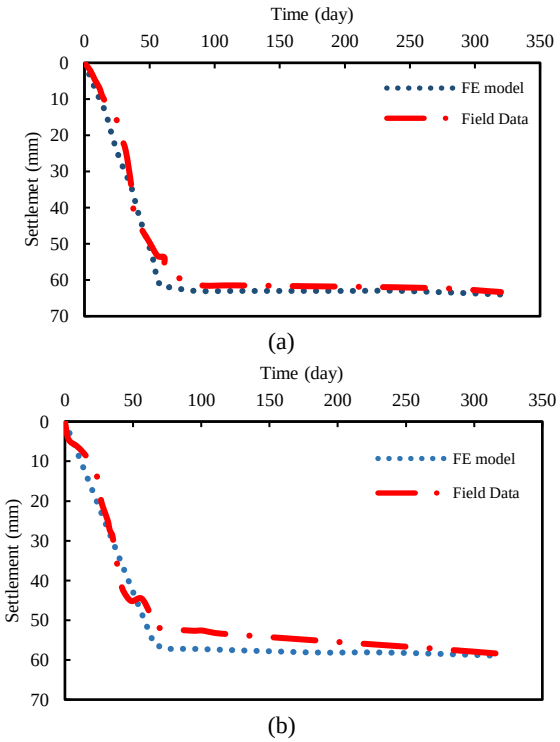

Figure 4. Measurements versus computed FE results: (a) settlement of the surface soil ; (b) settlement of the pile cap

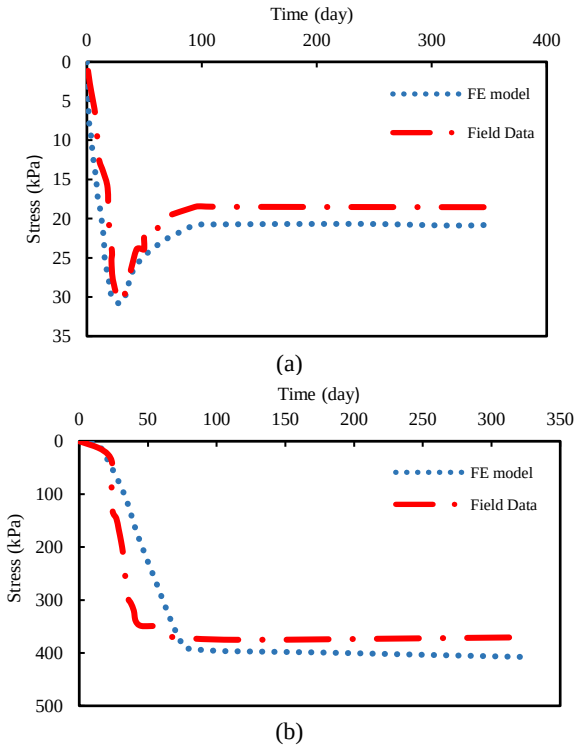

Figure 5. Measurements versus computed FE results: (a) Vertical stress of the surface soil; (b) Vertical stress of the pile cap

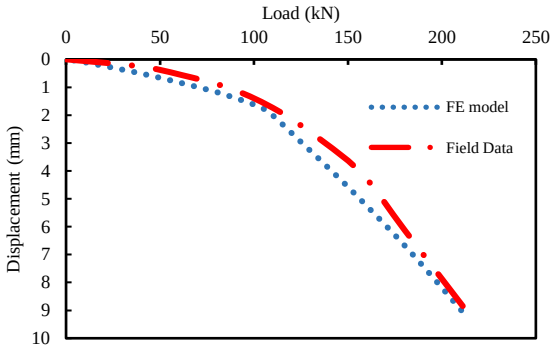

Figure 6. The displacement vs. load curves of the validation numerical model compared with the field compression test PA-1

4. RESULTS AND DISCUSSION

4. 1. Effect of the Size of Pile Caps Four modes were developed to study the effect of the presence of a cap and its dimensions and evaluate its performance in helical pile-supported embankments. Figure 7 evaluates the load transfer mechanism with efficiency and arching ratio parameters for different sizes of the pile caps. According to the results, the presence of caps and the rise in their size enhanced the load transfer mechanism in helical pile-supported embankments such that the pile

TABLE 3. Summary of the parameters used for model validation

Piled embankment (data from Chen et al. [41])						
Material	**γ (kN/m³)**	**E (MPa)**	**ν**	**C' (kPa)**	**ϕ' (degree)**	**e_0**
Embankment	21	15	0.30	0	32	-
ML	19.3	6.5	0.35	0	21	0.818
CL	16.7	2.4	0.30	0	24	1.286
GM	19.9	40	0.27	0	30	-
Pile and Cap	24.5	35000	0.15	-	-	-
Soil parameters (data from Elsherbiny and El Naggar . [29])						
Depth (m)	**γ (kN/m³)**	**E (MPa)**	**ν**	**ϕ' (degree)**	**ψ (degree)**	**-**
0-5	20	50	0.3	24	10	-
5-9	20	50	0.3	21	10	-

γ = Unit weight, E = Young's modules, ν = Poisson's ratio, C = Effective cohesion, ϕ′ = Effective friction Angle, ψ = Dilation Angle, e_0 = Void ratio

TABLE 4. Pile parameters used in validation models

Parameter	Helical pile (Elsherbiny and El Naggar (28))	Piled embankment (Chen et al. (40))
Shaft diameter (mm)	273	400
Length of pile (m)	5.5	20
Helix diameter (mm)	610	-
Number of helix	1	-
Thickness of the shaft (mm)	9.3	-
Thickness of the helix (mm)	20	-

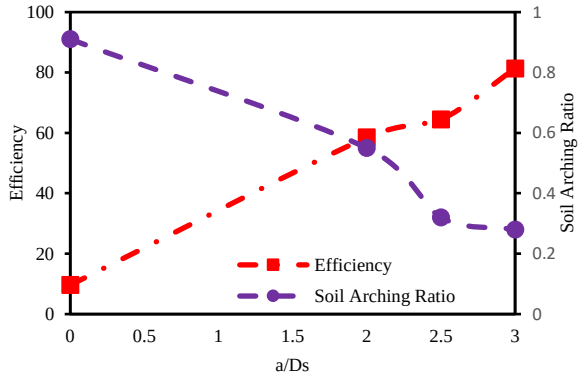

Figure 7. The load transfer mechanism for different a/D_s ratios of helical pile cap (a= cap width, D_s= shaft diameter)

cap efficiency and arching ratio improved to 88% and 69%, respectively, for a cap with a width of 1.5m compared to the mode with no cap.

As shown in Figure 7, the rise in the pile cap dimensions improved the load transfer mechanism in pile-supported embankments, resulting in the greater participation of the piles in sustaining the ultimate load of the embankment. Figure 8 depicts the axial force distribution along embedment depth for a helical pile with one helix connected to the pile shaft (the closest pile to the center of the embankment). Increasing the cap width enhanced the bearing capacity of the pile shaft and due to the higher load-bearing of the shaft, the load-bearing contribution of the helix connected to the shaft decreased. The load-bearing share of the helix, being 23.3% of the total load-bearing when no cap was used, reduced to 14.1% when a cap with a width of 1.5m was used (Table 5). Figure 9 indicates that the load-bearing contribution of the helix connected to the helical pile

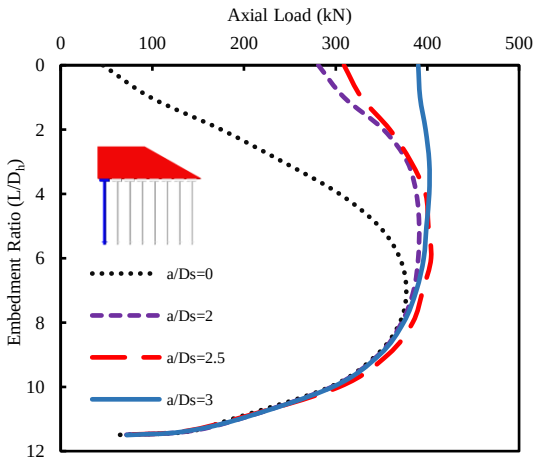

Figure 8. The axial load distribution along the embedment depth of piles for different a/D_s ratios of helical pile cap (a= cap width, D_s= shaft diameter)

TABLE 5. The load-bearing contribution of the helix and pile shaft for different ratios of cap width to helical pile shaft diameter, a/D_s.

Width Cap Ratio (a/Ds)	Portion of pile shaft (%)	Portion of helix (%)
0	76.7	23.3
2	82.3	17.7
2.5	83.4	16.6
3	85.9	14.1

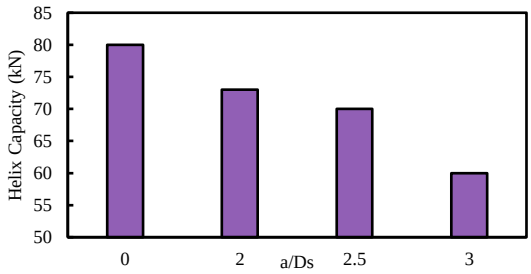

Figure 9. The load-bearing capacity of the helices connected to the pile shaft for different ratios of helical pile cap (a= cap width, D_s= shaft diameter)

shaft has increased with the reduction in the cap dimensions.

Besides enhancing the load-transfer mechanism in helical pile-supported embankments, adding caps to piles has reduced the vertical settlements of the embankment constructed on the soft soil. Figure 10 depicts the vertical displacement contours of the granular embankment, at the depth of 6 m of the embankment. The use of a cap with a width of 1 m reduced the vertical settlement of the embankment by 9.7% compared to the model with no cap on the pile. By increasing the cap width to 1.25m and 1.5m, the settlement reduced to 3.6% and 4%, respectively.

4. 2. Effect of the Wing Ratio The wing ratio is defined as the ratio of the helix diameter to the shaft diameter. In this parametric study, the fixed value of 1 m was considered for the helix diameter, while the pile shaft diameter varied. Figure 10 illustrates the variations in the efficiency and arching ratio against the shaft diameter. As shown in Figure 11, increasing the wing ratio decreases the load-bearing area and parameters of the load transfer mechanism. For example, increasing the wing ratio from 2 to 4 results in the growth of the arching ratio by 24% but reversely reduces the pile efficiency by 6.2%. On the other hand, by decreasing the wing ratio, the load-bearing area of the pile has increased, resulting in greater loads imposed on piles and improving the load transfer mechanisms. Reducing the wing ratio from 2 to 1.5 has

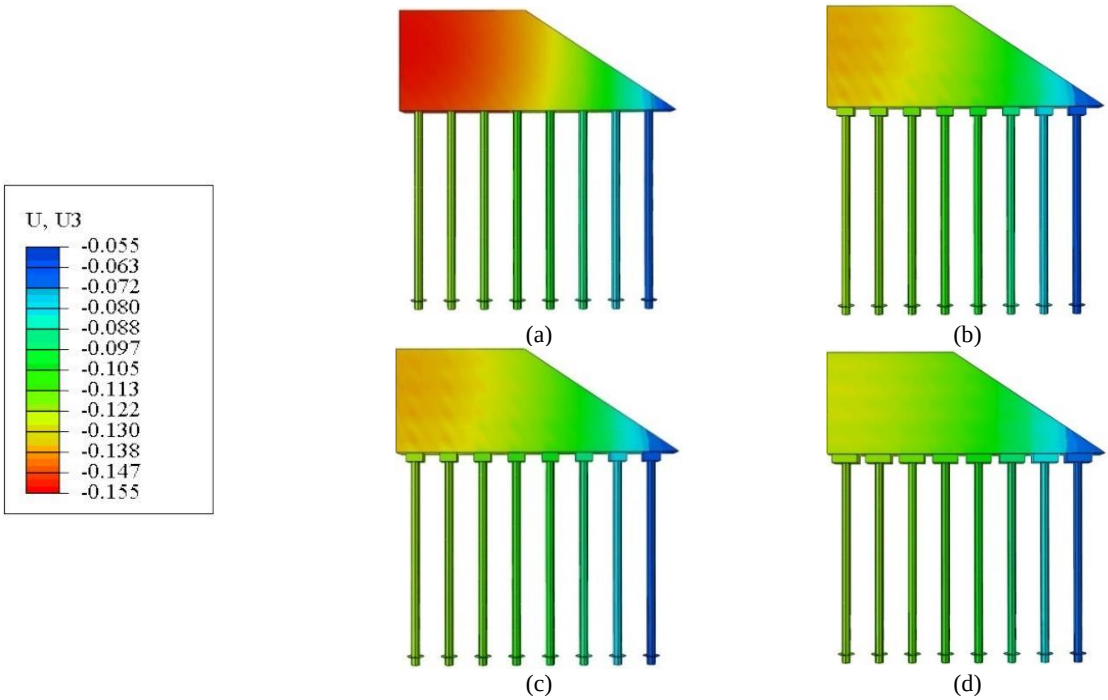

Figure 10. The vertical deformation contours of the granular embankment for different dimensions of the helical pile cap. a) without the cap, b) cap width = 1m, c) cap width = 1.25m, and d) cap width = 1.5m

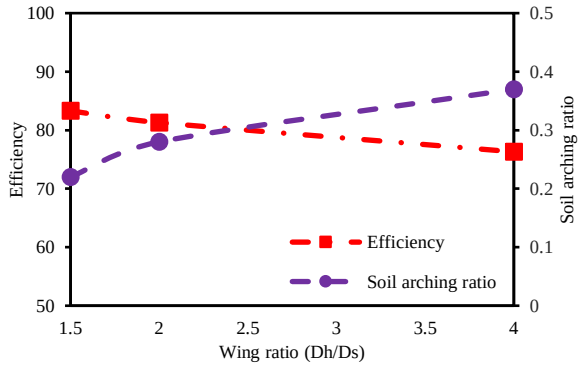

Figure 11. The load transfer mechanism for different wing ratios of the helical pile (D_h = helix diameter, D_s = shaft diameter)

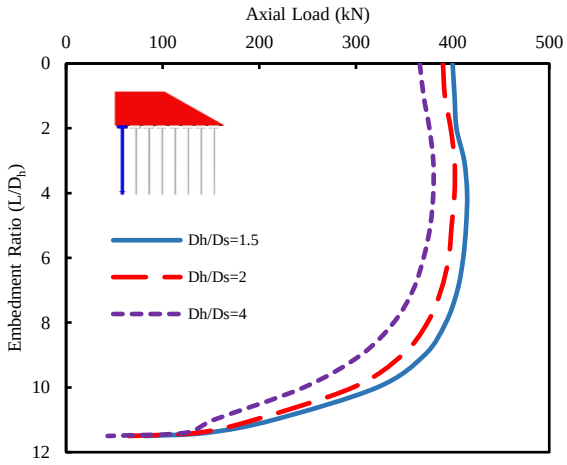

Figure. 12. The axial load distribution along the embedment depth of piles for different wing ratios of the helical pile (D_h = helix diameter, D_s = shaft diameter)

decreased the arching ratio by 24% while increasing the pile efficiency by 2.4%. The variations of axial load distribution along the embedment depth of the pile against wing ratio are plotted in Figure 12. With the reduction in the wing ratio (rise in the pile shaft diameter), the load-bearing area of the pile shaft has increased, causing to a higher axial force distribution along the pile length. Table 6 lists the load-bearing share of the pile shaft and helix. Based on the results presented in Figure 13, as the wing ratio decreases, the load-bearing area of the helix becomes smaller, leading to lower contribution against the imposed loads and less bearing capacity of the helix.

TABLE 6. The load-bearing contribution of the helix and pile shaft for different wing ratios of helical pile

Wing Ratio (D_h/D_s)	Portion of pile shaft (%)	Portion of helix (%)
1.5	85.6	14.4
2	83.7	16.3
4	80.5	19.5

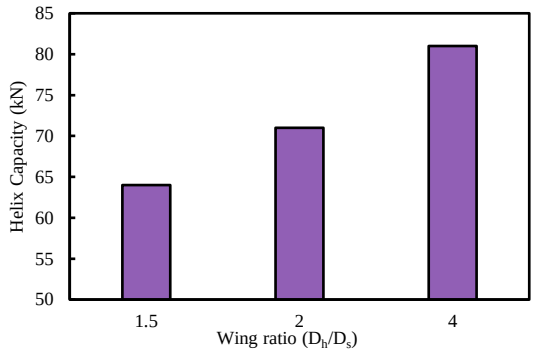

Figure 13. The load-bearing capacity of the helices connected to the pile shaft for different wing ratios of the helical pile

Figure 14 depicts the vertical displacement contours of the granular embankment against the wing ratio. The rise in the wing ratio means the reduction in shaft diameter, causing to reduction in soil-pile shaft resistance, and consequently, resulting in the rise in the vertical displacements of the embankment, as can be seen in Figure 14. Vertical displacement has decreased by 6.6% and 8.1% with a reduction in the wing ratio from 2 to 1.5 and from 4 to 2, respectively.

4. 3. Effect of the Spacing Ratio This section discusses effects of the the spacing between helices connected to a helical pile shaft, which is specified as the spacing ratio and defined as the ratio of the vertical distance between helices in the same pile to helix diameter. The 2- and 3-helix piles were modeled with spacing ratios of 1.5, 2.25, and 3. Figure 15 demonstrates the arching ratio and pile efficiency for different values of the spacing ratio. The results indicate that when the distance between the helices is 1.5 times the diameter of the helix, the helical pile shows cylindrical failure behavior, and the soil enclosed between the helices helps to improve the frictional resistance of the pile, so in this case, the maximum load is transferred to the piles as well as the load transfer mechanism increases. At the spacing ratio of 1.5, the 3-helix pile has reduced the arching ratio

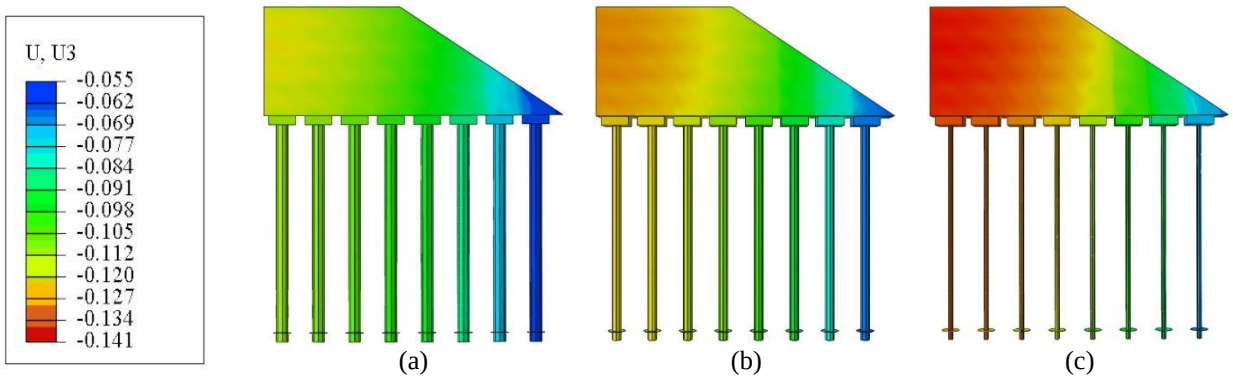

Figure 14. The vertical deformation contours of the granular embankment for different wing ratios of the helical pile; a) wing ratio = 1.5, b) wing ratio = 2, and c) wing ratio = 4

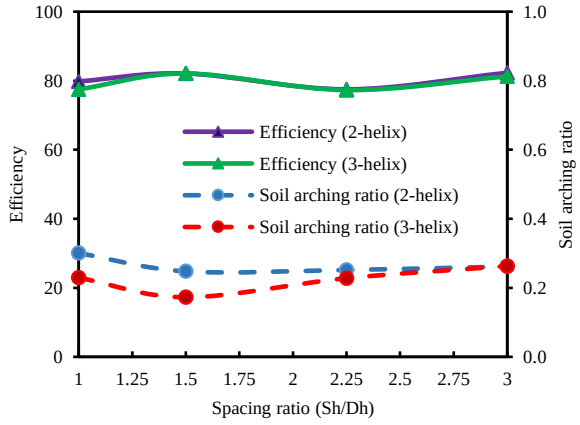

Figure 15. The load transfer mechanism for the different spacing ratios of the helical pile (S_h = vertical distance between helices , D_h=helix diameter)

by 30% compared to the 2-helix one, while its efficiency has not changed. Figure 15 demonstrates the total load-bearing capacities of the helices at different spacing ratios for the 2- and 3-helix piles. The reduction in the spacing ratio of the helices is leading to higher bearing capacity. Moreover, in the 3-helix pile, the total bearing capacity of the helices was higher than that of the 2-helix pile due to the helices' greater contribution to the total load-bearing. Figure 16 shows the load-bearing capacity of the helices connected to the pile shaft for different spacing ratios of the helical pile.

The vertical settlement of the embankment does not vary significantly with the increase in the number of helices or changes in their spacing ratio. Figure 17 shows the vertical displacement contours of the granular embankment for the 3-helix pile at different spacing ratios. Similar to the 3-helix pile, the 2-helix pile shows

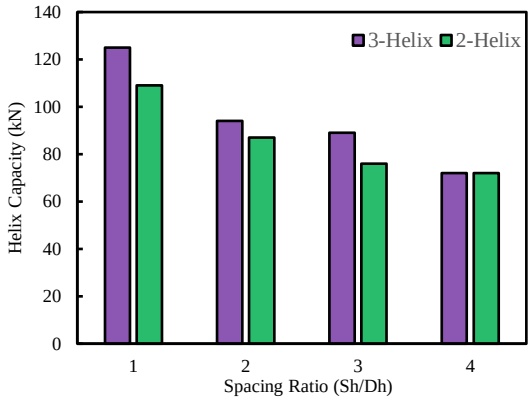

Figure 16. The load-bearing capacity of the helices connected to the pile shaft for different spacing ratios of the helical pile

no differences in vertical displacement at different spacing ratios. Accordingly, it can be concluded that adding helices to a helical pile does not remarkably affect the vertical displacements of a granular embankment. Table 7 lists the load-bearing contributions of the helices and pile shaft. According to the results, adding the third helix has reduced the load bearing of the upper helix and pile shaft. With increasing the spacing ratio of the helices, the pile had a separate load-bearing behavior resulting in a greater load-bearing contribution of the pile shaft. It can be concluded that regarding engineering uses and installation of helical piles, adding more than one helix to the pile shaft is not reasonable and does not significantly influence the vertical settlement of the pile-supported embankments. Thus, it is recommended to use helical piles with one helix connected to the shaft.

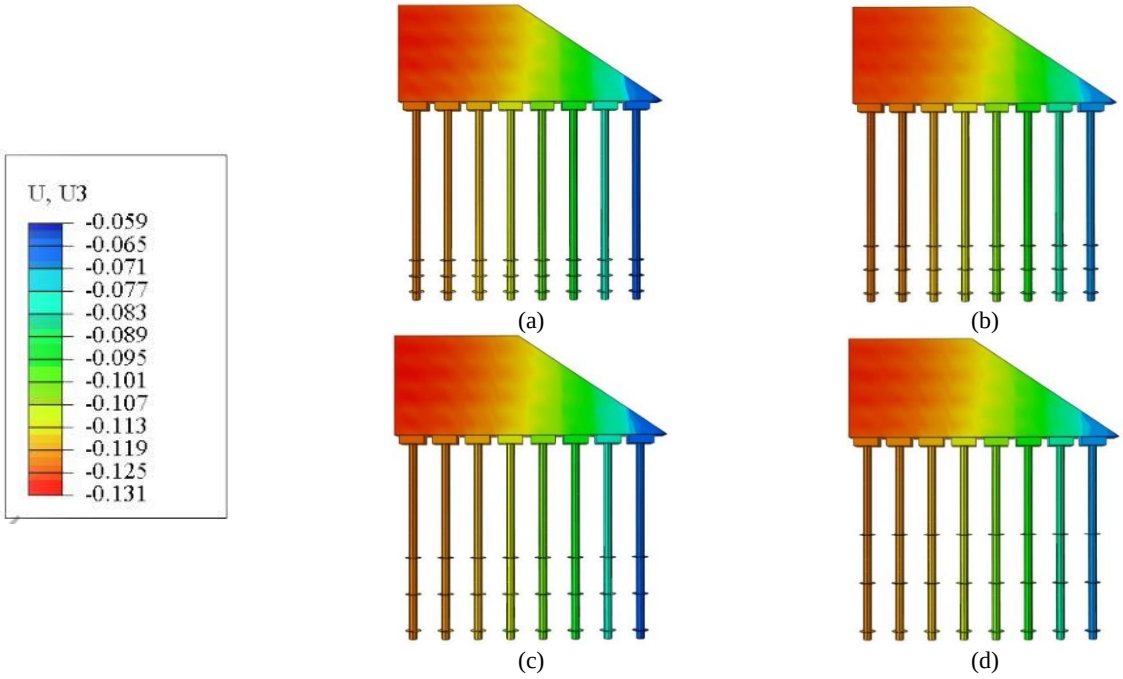

Figure 17. The vertical deformation contours of the granular embankment for different spacing ratios of the 3-helix piles. a) spacing ratio = 1, b) spacing ratio = 1.5, c) spacing ratio = 2.25, and d) spacing ratio = 3

TABLE 7. The load-bearing contribution of each helix and pile shaft for different spacing ratios of helical pile

No. Helix	Spacing ratio (S_h/D_h)	The portion of the pile shaft (%)	Portion of bottom helix (%)	Portion of Middle helix (%)	Portion of Top helix (%)
2	1	77.2	13.2	-	9.6
	1.5	81.1	13.1	-	5.9
	2.25	83.1	13.3	-	3.6
	3	84.1	12.8	-	3.1
3	1	73.9	12.7	9.2	4.2
	1.5	79.6	12.8	6.1	1.5
	2.25	80.8	11.9	6.5	0.8
	3	83.4	14	1.6	1

5. LIMITATIONS

(i) The current study deals with the use of cohesive-frictional materials possessing high frictional strength and coarse-grained soil for embankment fill which can largely remain in a relatively dry state. Therefore, the consolidation settlements are ignored in this study. However, consolidation can be a significant issue when dealing with saturated soft soils.
(ii) Considering the complexity of the problem investigated in this study and the difficulties in accurately determining the parameters for advanced soil models, the linearly elastic-perfectly plastic soil model with the Mohr-Coulomb strength criterion considering the dilation angle was used in this study.
(iii) The helix is idealized as a planner cylindrical disk. Therefore, modeling of the pile and surrounding soil can take advantage of the axisymmetric condition.

6. CONCLUSIONS

In the current study, the factors effective in the performance of helical pile-supported embankments were investigated in soft soils through FE modeling using ABAQUS software. The numerical models were validated using the field measurements on pile-supported embankments and helical pile loading in real dimensions. Afterward, a parametric study was performed to investigate the performance of helical pile-supported embankments. The following results are concluded based on the current study:
1. The results of the numerical modeling revealed that the performance of the helical piles in the pile-supported embankments depends on the cap dimensions. The vertical settlements could be reduced with the increase in the cap dimensions, and the load transfer mechanism could be improved due to the lower pressure on the soft soil surface and higher load distribution along the pile length. As a result, the load-bearing of the helices was decreased, and the pile shaft had a greater contribution to the load imposed on the pile.
2. The soil-pile interface showed a rise with the increase in the helical pile diameter, which led to the improved performance of the system and reduced settlements. Due to the greater contribution of the pile with the rise in the shaft diameter, the load transfer mechanism was improved. The evaluation of the load-bearing capacity of the pile revealed that with the rise in the pile diameter, the load-bearing capacity of the helices decreased, and a remarkable improvement occurred in the frictional capacity of the pile.
3. Evaluation of the results regarding the number and spacing of helices showed that adding helices can be ignored when controlling the vertical settlement of granular embankments is a concern. Also, cylindrical shear failure occurred when the spacing of the helices was 1.5 times the helix diameter, which increased the pile bearing capacity and improved the load transfer mechanism. The pile with three helices connected to the shaft had a better performance than the one with two helices. Moreover, adding helices to the helical pile and reducing the spacing of the helices could cause a reduction in the load-bearing contribution of the pile shaft, and increase the load-bearing contribution of the helices.
4. The major load of the pile throughout the modeling was carried by the pile shaft, while the contribution of the helices to the ultimate load bearing was almost 20%, on average. Therefore, the design of helical piles for pile-supported embankments should focus on the pile shaft. Therefore, piles with more than 1 helix are not recommended in terms of pile installation and economic conditions.

7. REFERENCES

1. Han J, Gabr M. Numerical analysis of geosynthetic-reinforced and pile-supported earth platforms over soft soil. Journal of geotechnical and geoenvironmental engineering. 2002;128(1):44-53. https://doi.org/10.1061/(ASCE)10900241(2002)128:1(44)
2. Chen R, Chen Y, Han J, Xu Z. A theoretical solution for pile-supported embankments on soft soils under one-dimensional compression. Canadian Geotechnical Journal. 2008;45(5):611-23. https://doi.org/10.1139/t08-003
3. Brohi AS, Saand A, Sahito ZA. 3D Numerical Modeling of Pile embankment performance on Soft Soil. International Journal. 2021;9(6). https://doi.org/10.30534/ijeter/2021/16962021
4. Zhang D, Zhang Y, Kim CW, Meng Y, Garg A, Garg A, et al. Effectiveness of CFG pile-slab structure on soft soil for supporting high-speed railway embankment. Soils and Foundations. 2018;58(6):1458-75. https://doi.org/10.1016/j.sandf.2018.08.007
5. Ding X, Luan L, Liu H, Zheng C, Zhou H, Qin H. Performance of X-section cast-in-place concrete piles for highway constructions over soft clays. Transportation Geotechnics. 2020;22:100310. https://doi.org/10.1016/j.trgeo.2019.100310
6. Briançon L, Simon B. Pile-supported embankment over soft soil for a high-speed line. Geosynthetics International. 2017;24(3):293-305. https://doi.org/10.1680/jgein.17.00002
7. Xu C, Song S, Han J. Scaled model tests on influence factors of full geosynthetic-reinforced pile-supported embankments. Geosynthetics International. 2016;23(2):140-53. https://doi.org/10.1680/jgein.15.00038
8. Fagundes DF, Almeida MS, Thorel L, Blanc M. Load transfer mechanism and deformation of reinforced piled embankments. Geotextiles and Geomembranes. 2017;45(2):1-10. https://doi.org/10.1016/j.geotexmem.2016.11.002
9. Zhao M, Liu C, El-Korchi T, Song H, Tao M. Performance of geogrid-reinforced and PTC pile-supported embankment in a highway widening project over soft soils. Journal of Geotechnical and Geoenvironmental Engineering. 2019;145(11):06019014. https://doi.org/10.1061/(ASCE)GT.1943-5606.0002157

10. Lee T, Lee S, Lee I-W, Jung Y-H. Quantitative performance evaluation of GRPE: a full-scale modeling approach. Geosynthetics International. 2020;27(3):342-7. https://doi.org/10.1680/jgein.19.00017
11. Bangia T, Raskar R. Cohesive methodology in construction of enclosure for 3.6 m devasthal optical telescope. HighTech and Innovation Journal. 2022;3(2):162-74. https://doi.org/10.28991/HIJ-2022-03-02-05
12. Lu W, Miao L, Wang F, Zhang J, Zhang Y, Wang H. A case study on geogrid-reinforced and pile-supported widened highway embankment. Geosynthetics International. 2020;27(3):261-74. https://doi.org/10.1680/jgein.19.00024
13. Wu P-C, Feng W-Q, Yin J-H. Numerical study of creep effects on settlements and load transfer mechanisms of soft soil improved by deep cement mixed soil columns under embankment load. Geotextiles and Geomembranes. 2020;48(3):331-48. https://doi.org/10.1016/j.geotexmem.2019.12.005
14. Phutthananon C, Jongpradist P, Jongpradist P, Dias D, Baroth J. Parametric analysis and optimization of T-shaped and conventional deep cement mixing column-supported embankments. Computers and Geotechnics. 2020;122:103555. https://doi.org/10.1016/j.compgeo.2020.103555
15. Bahrami M, Marandi S. Large-scale experimental study on collapsible soil improvement using encased stone columns. International Journal of Engineering, Transactions B: Applications, . 2021;34(5):1145-55. https://doi.org/10.5829/ije.2021.34.05b.08
16. Pham TA. Design and analysis of geosynthetic-reinforced and floating column-supported embankments. International Journal of Geotechnical Engineering. 2022;16(10):1276-92. https://doi.org/10.1080/19386362.2021.1997209
17. Umravia N, Solanki CH. Numerical Analysis to Study Lateral Behavior of Cement Fly Ash Gravel Piles under the Soft Soil. International Journal of Engineering, Transactions B: Applications,. 2022;35(11):2111-9. https://doi.org/10.5829/ije.2022.35.11b.06
18. Ye X, Wu J, Li G. Time-dependent field performance of PHC pile-cap-beam-supported embankment over soft marine clay. Transportation Geotechnics. 2021;26:100435. https://doi.org/10.1016/j.trgeo.2020.100435
19. Wu J, Ye X, Li J, Li G. Field and numerical studies on the performance of high embankment built on soft soil reinforced with PHC piles. Computers and Geotechnics. 2019;107:1-13. https://doi.org/10.1016/j.compgeo.2018.11.019
20. Ahmed D, bt Taib SNL, Ayadat T, Hasan A. Numerical analysis of the carrying capacity of a piled raft foundation in soft clayey soils. Civil Engineering Journal. 2022;8(04). https://doi.org/10.28991/CEJ-2022-08-04-01
21. Liu K-F, Feng W-Q, Cai Y-H, Xu H, Wu P-C. Physical model study of pile type effect on long-term settlement of geosynthetic-reinforced pile-supported embankment under traffic loading. Transportation Geotechnics. 2023;38:100923. https://doi.org/10.1016/j.trgeo.2022.100923
22. Lutenegger AJ. Historical development of iron screw-pile foundations: 1836–1900. The International Journal for the History of Engineering & Technology. 2011;81(1):108-28. https://doi.org/10.1179/175812109X12547332391989
23. Sakr M. Performance of helical piles in oil sand. Canadian Geotechnical Journal. 2009;46(9):1046-61. https://doi.org/10.1139/t09-044
24. Spagnoli G, de Hollanda Cavalcanti Tsuha C. A review on the behavior of helical piles as a potential offshore foundation system. Marine Georesources & Geotechnology. 2020;38(9):1013-36. https://doi.org/10.1080/1064119X.2020.1729905
25. Elkasabgy M, El Naggar MH. Axial compressive response of large-capacity helical and driven steel piles in cohesive soil. Canadian Geotechnical Journal. 2015;52(2):224-43. https://doi.org/10.1139/cgj-2012-0331
26. Alwalan M, Alnuaim A. Axial Loading Effect on the Behavior of Large Helical Pile Groups in Sandy Soil. Arabian Journal for Science and Engineering. 2022;47(4):5017-31. https://doi.org/10.1007/s13369-021-06422-9
27. Nowkandeh MJ, Choobbasti AJ. Numerical study of single helical piles and helical pile groups under compressive loading in cohesive and cohesionless soils. Bulletin of Engineering Geology and the Environment. 2021;80:4001-23. https://doi.org/10.1007/s10064-021-02158-w
28. Elsherbiny ZH, El Naggar MH. Axial compressive capacity of helical piles from field tests and numerical study. Canadian Geotechnical Journal. 2013;50(12):1191-203. https://doi.org/10.1139/cgj-2012-0487
29. Terzaghi K. Theoretical soil mechanics1943.
30. Hewlett W, Randolph M, editors. Analysis of piled embankments. International journal of rock mechanics and mining sciences and geomechanics abstracts; 1988: Elsevier Science.
31. Tang SK. Arching in piled embankments 1992.
32. Le Hello B, Villard P. Embankments reinforced by piles and geosynthetics—Numerical and experimental studies dealing with the transfer of load on the soil embankment. Engineering geology. 2009;106(1-2):78-91. https://doi.org/10.1016/j.enggeo.2009.03.001
33. Bhasi A, Rajagopal K. Numerical study of basal reinforced embankments supported on floating/end bearing piles considering pile–soil interaction. Geotextiles and Geomembranes. 2015;43(6):524-36. https://doi.org/10.1016/j.geotexmem.2015.05.003
34. Ariyarathne P, Liyanapathirana D. Review of existing design methods for geosynthetic-reinforced pile-supported embankments. Soils and Foundations. 2015;55(1):17-34. https://doi.org/10.1016/j.sandf.2014.12.002
35. Meena NK, Nimbalkar S, Fatahi B, Yang G. Effects of soil arching on behavior of pile-supported railway embankment: 2D FEM approach. Computers and Geotechnics. 2020;123:103601. https://doi.org/10.1016/j.compgeo.2020.103601
36. Pham TA, Dias D. 3D numerical study of the performance of geosynthetic-reinforced and pile-supported embankments. Soils and Foundations. 2021;61(5):1319-42. https://doi.org/10.1016/j.sandf.2021.07.002
37. Al-Tememy M, Al-Neami M, Asswad M. Finite element analysis on behavior of single battered pile in sandy soil under pullout loading. International Journal of Engineering, Transactions C: Aspects. 2022;35(6):1127-34. https://doi.org/10.5829/ije.2022.35.06c.04
38. Khanmohammadi M, Fakharian K. Evaluation of performance of piled-raft foundations on soft clay: A case study. Geomechanics and Engineering. 2018;14(1):43-50. https://doi.org/10.12989/gae.2018.14.1.043
39. Shawky O, Altahrany AI, Elmeligy M. Study of lateral load influence on behaviour of negative skin friction on circular and square piles. Civil Engineering Journal. 2022;8(10):2125-53. https://doi.org/10.28991/CEJ-2022-08-10-08
40. Chen R, Xu Z, Chen Y, Ling D, Zhu B. Field tests on pile-supported embankments over soft ground. Journal of Geotechnical and Geoenvironmental Engineering. 2010;136(6):777-85. https://doi.org/10.1061/(ASCE)GT.1943-5606.0000295

Persian Abstract

چکیده

جستجو برای راه‌حل‌های عملی و اقتصادی برای افزایش پایداری و کاهش نشست‌های کلی و تفاضلی خاکریزها ضروری است. امروزه استفاده از المان‌های سازه‌ای مانند شمع‌ها، به عنوان یک راه‌حل مؤثر در بهبود عملکرد کلی یک سیستم خاکریزی در نظر گرفته می‌شوند. در سال‌های اخیر استفاده از شمع‌های مارپیچ به دلیل عملکرد مناسب تحت بار فشاری و کششی، نصب سریع و آسان شمع و حذف مشکلات بتن‌ریزی مورد توجه قرار گرفته است. هدف در این مقاله بررسی و شناخت رفتار خاکریزهای متکی بر شمع‌های مارپیچ است که به‌همین منظور یک مطالعه عددی سه‌بعدی با استفاده از نرم‌افزار آباکوس توسعه داده شد. صحت‌سنجی باتوجه به گزارش‌های میدانی و آزمایشگاهی گزارش شده توسط دیگر محققان انجام شد و در ادامه مدل‌های عددی سه‌بعدی به‌منظور بررسی اثرات کلاهک شمع، نسبت قطر پره به قطر شفت، تعداد پره‌ها و فاصله بهینه بین پره‌ها توسعه داده شد. نتایج نشان می‌دهد افزایش پره‌ها و تغییر فاصله بین آن‌ها تاثیری بر میزان کنترل نشست نخواهد داشت. همچنین پارامترهای مکانیزم انتقال بار با افزایش ابعاد کلاهک و قطر شفت شمع ارتباط مستقیم دارد. اضافه کردن پره به شمع ظرفیت باربری شمع را افزایش می‌دهد که در نتیجه باعث می‌شود پارامترهای مکانیزم انتقال بار بهبود یابد، به‌طوریکه در شمع مارپیچ با ۳ پره نسبت قوس زدگی تا ٤٠ درصد نسبت با شمعی با ۱ پره کاهش می‌یابد. همچنین نتایج نشان می‌دهد به طور میانگین ۸۰ درصد سهم بار وارد بر شمع را شفت تحمل می‌کند و پره تاثیری کمتری بر عملکرد خاکریزهای متکی بر شمع خواهد داشت.